

Bandwidth and Gain Enhancement of MIMO Antenna by Using Ring and Circular Parasitic with Air-Gap Microstrip Structure

Teguh Firmansyah^{*1}, Herudin², Suhendar³, Romi Wiryadinata⁴, M. Iman Santoso⁵,
Yus Rama Denny⁶, Toto Supriyanto⁷

^{1,2,3,4,5}Department of Electrical Engineering, University of Sultan Ageng Tirtayasa, Cilegon 42435

⁶Department of Physics Education, University of Sultan Ageng Tirtayasa, Serang 42124

⁷Department of Electrical Engineering, Jakarta State Polytechnic, Depok 16424

*Corresponding author, e-mail: teguhfirmansyah@untirta.ac.id

Abstract

This research was proposed a circular patch MIMO antenna by using a ring and circular parasitic radiator structure. As a novelty, in order to enhance bandwidth and gain of circular patch MIMO antenna, a conventional circular patch MIMO antenna will be added a ring and a circular parasitic. Therefore, this research was investigated a conventional MIMO antenna (C-MA), ring parasitic MIMO antenna (RP-MA), and circular parasitic MIMO antenna (CP-MA) as Model 1, Model 2, and Model 3, respectively. This MIMO antenna was designed on FR4 microstrip substrate with $\epsilon_r = 4.4$, thickness $h = 1.6$ mm, and $\tan \delta = 0.0265$. This MIMO antenna has center frequency 2.35 GHz which is a frequency band for LTE application in Indonesia. An Advance Design System (ADS) software was used to determine the antenna parameters. The MIMO antenna C-MA / RP-MA/ CP-MA achieves 2.36GHz/ 2.38GHz/ 2.38 GHz, 70 MHz/ 100 MHz/ 120 MHz, 1.625 dBi/ 4.066 dBi/ 4.117 dBi, 6.414 dBi/ 7.26 dBi/ 7.153 dBi, 33.9 %/ 47.8 %/ 49.70 %, -12.35 dB/ -22.21 dB/ -23.66 dB, and -30.924 dB/ -28.46 dB/ -27.59 dB for center frequency, bandwidth, gain, directivity, efficiency, reflection coefficient, and mutual coupling, respectively. Compared to C-MA (Model 1) performances, The result showed that proposed antenna has wider-bandwidth/ higher-gain with 42.8%/ 150.2 %, and 71.4%/ 163.3% for RP-MA (Model 2) and CP-MA (Model 3), respectively. The proposed antenna has size of 50 mm x 130 mm x 23.2 mm. Measured results are in a good agreement with the simulated results.

Keywords: Antenna, MIMO, ring parasitic, circular parasitic

Copyright © 2017 Universitas Ahmad Dahlan. All rights reserved.

1. Introduction

A Long Term Evolution (LTE) technology was developed to provide the requirement of wireless data access with high bit-rate [1, 2]. The LTE technology uses a Multiple Input Multiple Output (MIMO) antenna system [3-5]. Antennas based on microstrip technology are popularly used because it has many benefits such as low cost, low profile, ease fabrication, and compact [6, 7]. However, the microstrip antenna has disadvantages such as narrow bandwidth and low gain [8, 9]. There are some attractive methods frequently used to enhance bandwidth and gain such as microstrip-slot [10-12], microstrip notch [13], and parasitic air gap [14-19]. The research which proposed by [10], [12-13] increases the bandwidth of the antenna, without gain enhancement. Some antenna mentioned above still a relatively complex geometry. A parasitic gap method which proposed by [14-19] are an excellent method. That method was not only to increase bandwidth but also enhance a gain. Unfortunately, these studies are only applied to a single patch antenna, not a MIMO antenna. MIMO antenna system is considered not only a bandwidth, and a gain but also a mutual coupling. A frequently used method to reduce a mutual coupling such as defected ground structure (DGS) [20], Electromagnetic band gap (EBG) [21], and Metamaterial mushroom structures. These methods made more complicated designs of MIMO antenna.

As a novelty, this research proposed a circular patch MIMO. In order to enhance bandwidth and gain, a conventional circular patch MIMO antenna will be added a ring and a circular parasitic radiator structure. Therefore, generally this research was investigated a conventional MIMO antenna (C-MA), ring parasitic MIMO antenna (RP-MA), and circular

parasitic MIMO antenna (CP-MA) as Model 1, Model 2, and Model 3, respectively. This MIMO antenna was designed on FR4 microstrip substrate with $\epsilon_r= 4.4$, thickness $h=1.6$ mm, and $\tan \delta= 0.0265$. This MIMO antenna has center frequency of 2.35 GHz, which is a frequency band for LTE application in Indonesia. A performance of MIMO antenna will be investigated include center frequency, bandwidth, gain, directivity, efficiency, reflection coefficient, and mutual coupling. The design of methodology was detailed in the following sections. Section 2 describes the design of a circular patch MIMO antenna by using a ring and circular parasitic radiator structure. The simulation was described in Section 3, and the measurement results of the MIMO antenna was described in Section 4. Finally, Section 4 concludes this research.

2. Research Method

This part discusses some methods to conduct the research. Figure 1(a) shows a circular patch conventional MIMO antenna (C-MA) [Model 1]. Figure 1(b) shows circular patch MIMO antenna with a ring-parasitic substrate (RP-MA) [Model 2]. Furthermore, Figure 1(c) shows circular patch MIMO antenna with a circular-parasitic substrate (CP-MA) [Model 3].

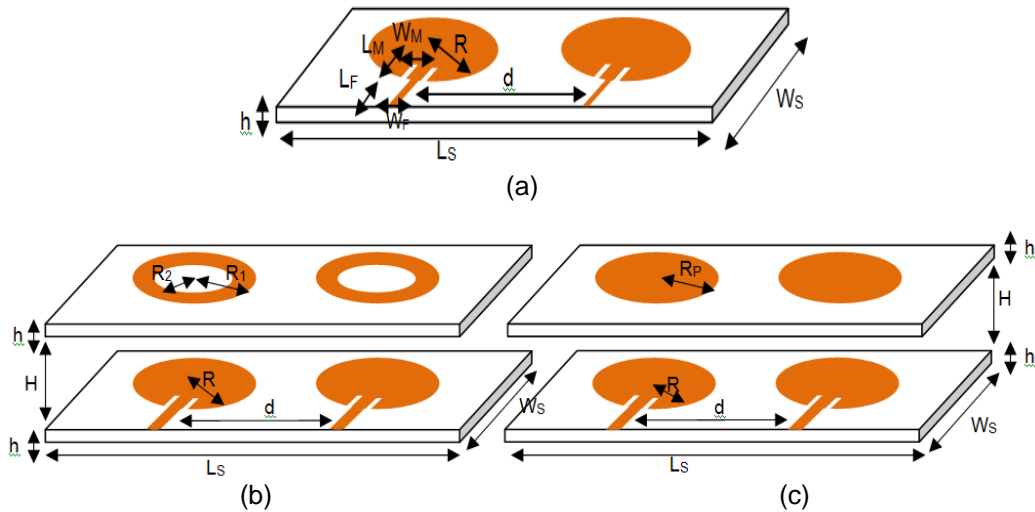


Figure 1. (a) Conventional MIMO antenna (C-MA) [Model 1], (b) MIMO antenna with ring parasitic substrate (RP-MA) [Model 2], (c) MIMO antenna with circular parasitic substrate (CP-MA) [Model 3]

The radius of circular patch microstrip antenna is given by [22]:

$$R = \frac{F}{\sqrt{1 + \frac{2h}{\pi\epsilon_r} \left[\ln\left(\frac{\pi F}{2h}\right) + 1.7726 \right]}} \tag{1}$$

Where,

$$F = \frac{8.791 \times 10^9}{f_r \sqrt{\epsilon_r}} \tag{2}$$

With h = thickness of substrate (cm) and f_r = resonant frequency (Hz).

In this research, a direct feeding method was used. The relationship between width-thickness (W/h) ratio of the feeding size and the value of Z_0 and the constant dielectric ϵ_r can be obtained by Equation (3) [23-25]:

$$\frac{W}{h} = \begin{cases} \frac{8e^A}{e^{2A}-2} & \text{for, } (W/h < 2) \\ \frac{2}{\pi} \left[B - 1 - \ln(2B - 1) + \frac{\epsilon_r - 1}{2\epsilon_r} \left\{ \ln(B - 1) + 0,39 - \frac{0,61}{\epsilon_r} \right\} \right] & \text{for, } (W/h > 2) \end{cases} \quad (3)$$

Where:

$$A = \frac{Z_0}{60} \sqrt{\frac{\epsilon_r + 1}{2}} + \frac{\epsilon_r - 1}{\epsilon_r + 1} \left\{ 0,23 + \frac{0,11}{\epsilon_r} \right\} \quad (4)$$

$$B = \frac{377\pi}{2Z_0\sqrt{\epsilon_r}} \quad (5)$$

Furthermore, the Z_0 can be determined by the ratio of width and thickness (W/h) [23-27]:

$$Z_0 = \begin{cases} \frac{60}{\sqrt{\epsilon_e}} \ln\left(\frac{8h}{W} + \frac{W}{4h}\right) & \text{for } (W/h \leq 1) \\ \frac{120\pi}{\sqrt{\epsilon_e} \left[\frac{W}{h} + 1,393 + 0,667 \ln\left(\frac{W}{h} + 1,444\right) \right]} & \text{for } (W/h \geq 1) \end{cases} \quad (6)$$

where:

$$\epsilon_e = \frac{\epsilon_r + 1}{2} + \frac{\epsilon_r - 1}{2} \frac{1}{\sqrt{1 + 12h/W}} \quad (7)$$

This MIMO antenna was designed on FR4 microstrip substrate with $\epsilon_r = 4.4$, thickness $h = 1.6$ mm, and $\tan \delta = 0.0265$. An Advance Design System (ADS) software was used to determine the antenna parameters. Figure 2(a) shows the extracted reflection coefficient and mutual coupling values with varied R_2 . The chart shows that the reflection coefficient can be tuned by modifying R_2 . It also can be seen that the mutual coupling values are still below -20 dB for all values of R_2 . Furthermore, Figure 2(b) shows the extracted reflection coefficient and mutual coupling values with varied R_p . It shows that R_p only significant affect to reflection coefficient, with less effect on mutual coupling.

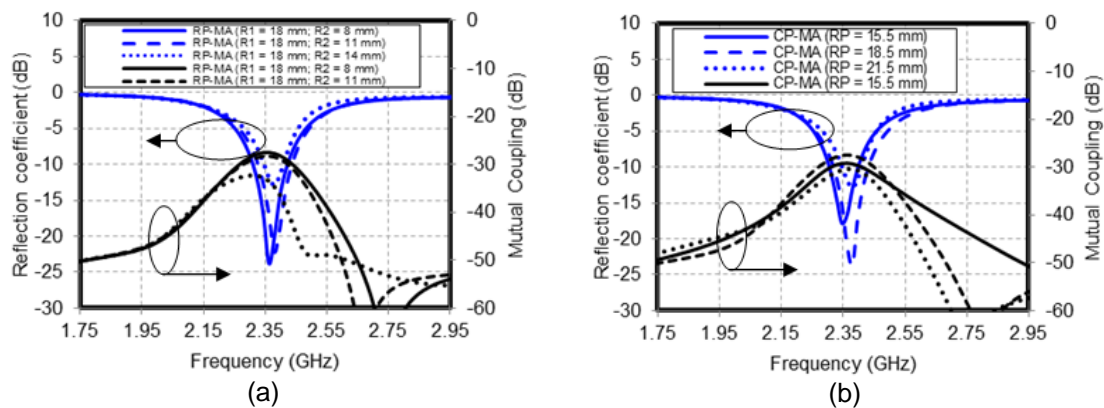


Figure 2. (a) The extracted reflection coefficient and mutual coupling values with varied R_2 ; (b) The extracted reflection coefficient and mutual coupling values with varied R_p

Figure 3(a) shows the extracted reflection coefficient with different distance between antennas d (mm). The chart reveals that the value of reflection coefficient at the center frequency lower than -10 dB. This result indicates that the distance d (mm) does not influence the center frequency. Figure 3(b) shows that the extracted mutual coupling with varied d (mm). These results determine that the smaller the antenna distance would be higher the coupling value.

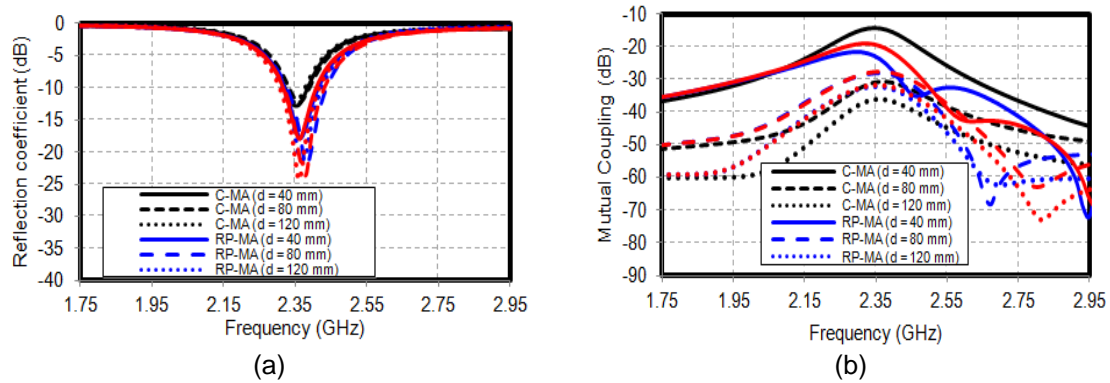


Figure 3. (a) The extracted reflection coefficient with varied distance d (mm); (b) The extracted mutual coupling with varied distance d (mm).

Figure 4(a) shows the extracted reflection coefficient with a variable distance between antennas and radiator H (mm). These results show that the various distance (H) will shift a center frequency. Moreover, the reflection coefficient at the center frequency is still lower than -10 dB. Otherwise, Figure 4(b) illustrated the mutual extraction coupling with different distance between antennas and radiator H (mm). The H is varied from 10 mm to 30 mm. It shows that the variation of H affected to mutual coupling values but still good isolation.

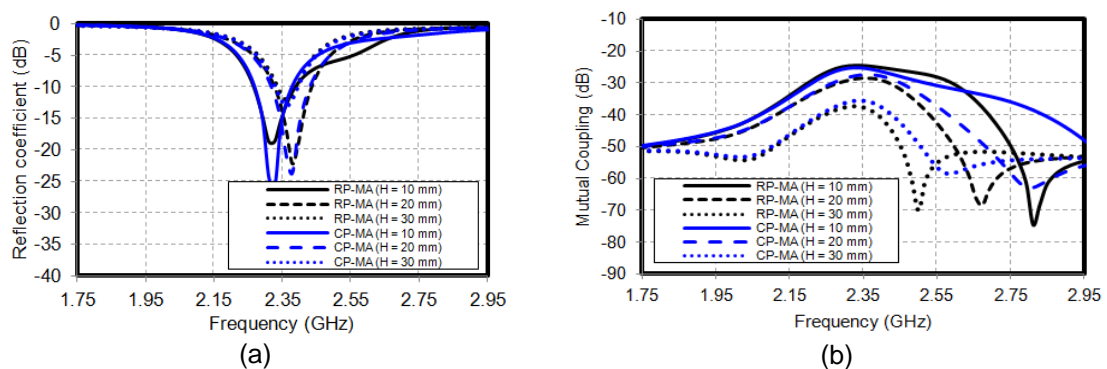


Figure 4. (a) The extracted reflection coefficient with varied distance H (mm); (b) The extracted mutual coupling with varied distance H (mm)

3. Results and Analysis

We organize the circular patch MIMO antenna by using a ring and circular parasitic radiator by special structure as depicted by Figure 1. The size of MIMO antenna are $L_S = 130$ mm, $W_S = 50$ mm, $L_F = 7.1$ mm, $W_F = 3$ mm, $L_M = 7.9$ mm, $W_M = 1$ mm, $R = 18.5$ mm, $h = 1.6$ mm, $d = 80$ mm, $R_1 = 18$ mm, $R_2 = 11$ mm, $H = 20$ mm, $R_P = 18.5$ mm. This MIMO antenna was designed on FR4 microstrip substrate with $\epsilon_r = 4.4$, thickness $h = 1.6$ mm, and $\tan \delta = 0.0265$. An Advance Design System (ADS) software was used to determine the antenna parameters. Vector Network Analyzer Agilent N9913A-210 was used to test an antenna performances. Furthermore, the photograph of fabricated antenna was shown in Figure 5.

Figure 6(a) and Figure 6(b) shows a comparison between simulated and measured of reflection coefficient and mutual coupling of circular patch MIMO antenna by using a ring and circular parasitic radiator structure. The C-MA antenna [Model-1] achieves center frequency = 2.36 GHz, bandwidth = 70 MHz, reflection coefficient = -12.35 dB, mutual coupling = -30.92 dB. The RP-MA antenna [Model-2] achieves simulated/measured of center frequency = 2.38 GHz/2.36 GHz, bandwidth = 100 MHz/100 MHz, reflection coefficient = -22.21 dB/ -15.93 dB, mutual coupling = -28.46 dB/-28.83 dB. The CP-MA antenna [Model-3] achieves

simulated/measured of center frequency = 2.38 GHz/2.36 GHz, bandwidth = 120 MHz/110 MHz, reflection coefficient = -23.66 dB/ -24.89 dB, mutual coupling = -27.59 dB/-31.67 dB. A good agreement can be observed between the simulated and measured results, which demonstrates the validity of the design.

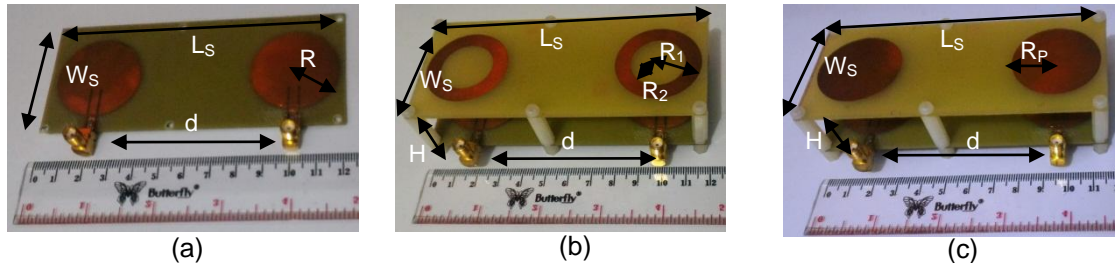


Figure 5. (a) Photograph of conventional MIMO antenna (C-MA) [Model 1], (b) Photograph of MIMO antenna with ring parasitic substrate (RP-MA) [Model 2], (c) Photograph of MIMO antenna with circular parasitic substrate (CP-MA) [Model 3]

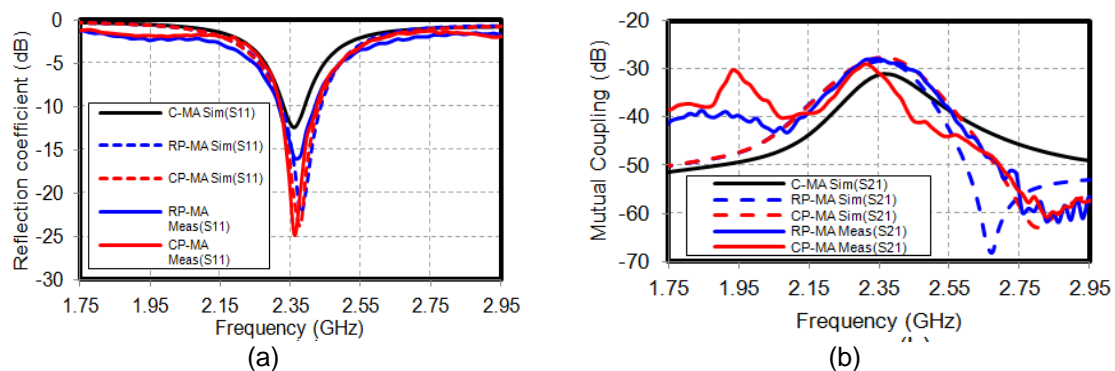


Figure 6. (a) The comparison between simulated and measured of reflection coefficient; (b) The comparison between simulated and measured of mutual coupling

Figure 7(a) shows the extracted gain and reflection coefficient with varied distance H (mm). In this research, the distance $H = 20$ mm was used which produce high gain with good reflection coefficient, simultaneously. Figure 7(b) shows that MIMO antenna with additional a ring and a circular parasitic radiator structure has higher gain compare to conventional MIMO antenna. Figure 7(c) and Figure 7(d) show a directivity and efficiency, respectively. The charts show that a directivity and efficiency of MIMO antenna with a ring and a circular parasitic radiator structure has higher value compare to conventional MIMO antenna.

Figure 8(a) displays the surface current distribution of circular antenna. The surface current distribution flowed only at the circular patch. Furthermore, Figure 8(b) shows the surface current distribution of circular antenna with parasitic ring substrate. The surface current distribution flowed not only at the circular patch but also at parasitic ring substrate. Moreover, Figure 8(c) shows the surface current distribution of circular antenna with circular parasitic substrate. The surface current distribution was flowed not only at the circular patch but also at circular parasitic substrate.

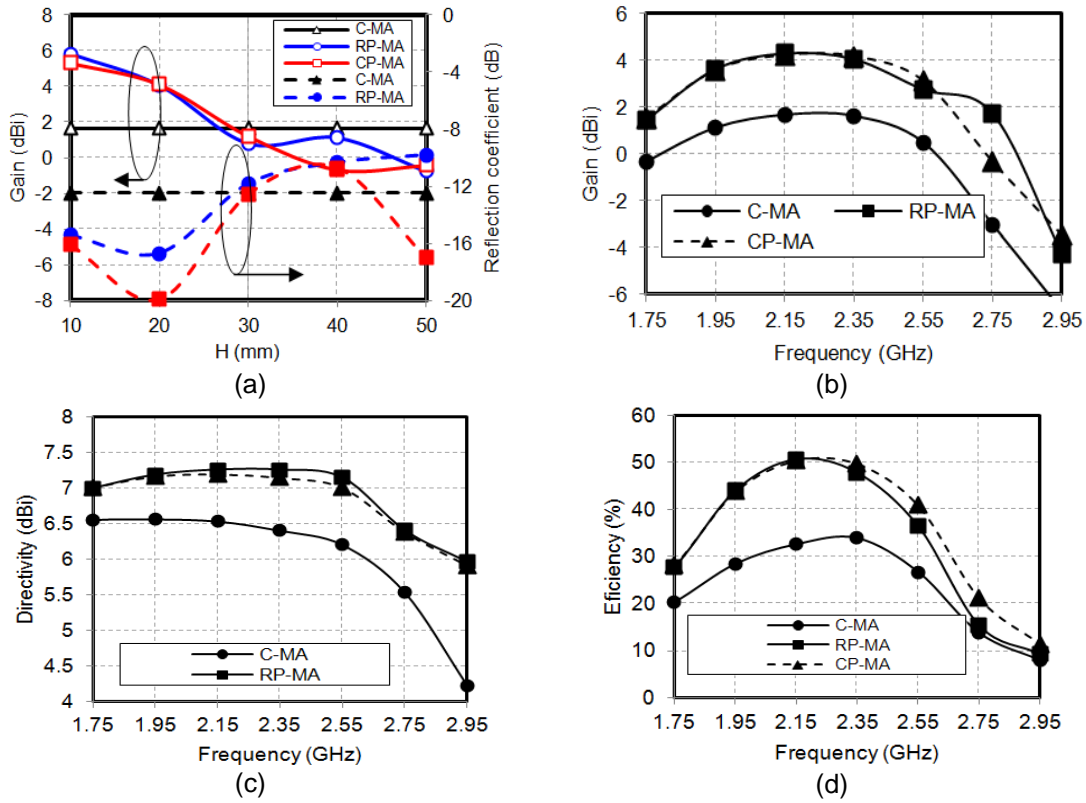


Figure 7. (a) The extracted gain and reflection coefficient with varied distance H (mm), (b) The comparison of gain (dBi), (c) The comparison of directivity (dBi), (d) The comparison of efficiency (%)

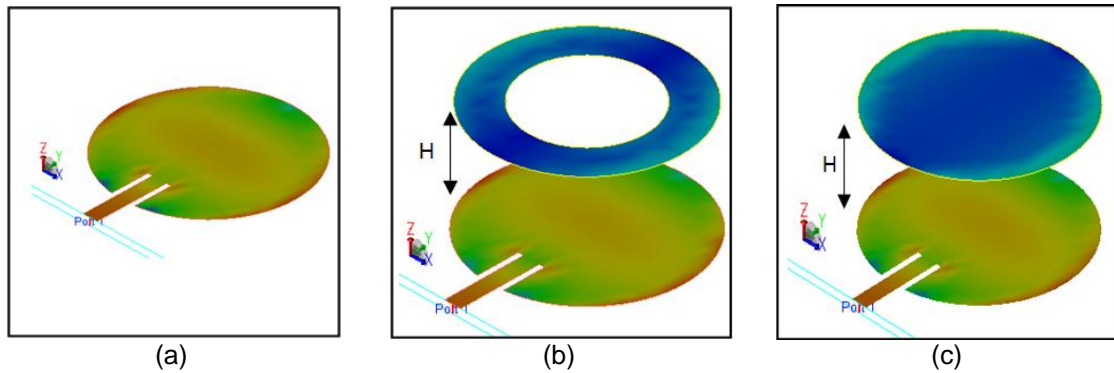


Figure 8. (a) The surface current distribution of circular antenna, (b) The surface current distribution of circular antenna with ring parasitic substrate, (c) The surface current distribution of circular antenna with circular parasitic substrate

Figure 9(a), Figure 9(b), and Figure 9(c) expose radiation pattern of conventional MIMO antenna (C-MA) [Model 1], MIMO antenna with ring parasitic substrate (RP-MA) [Model 2] and MIMO antenna with circular parasitic substrate (CP-MA) [Model 3].

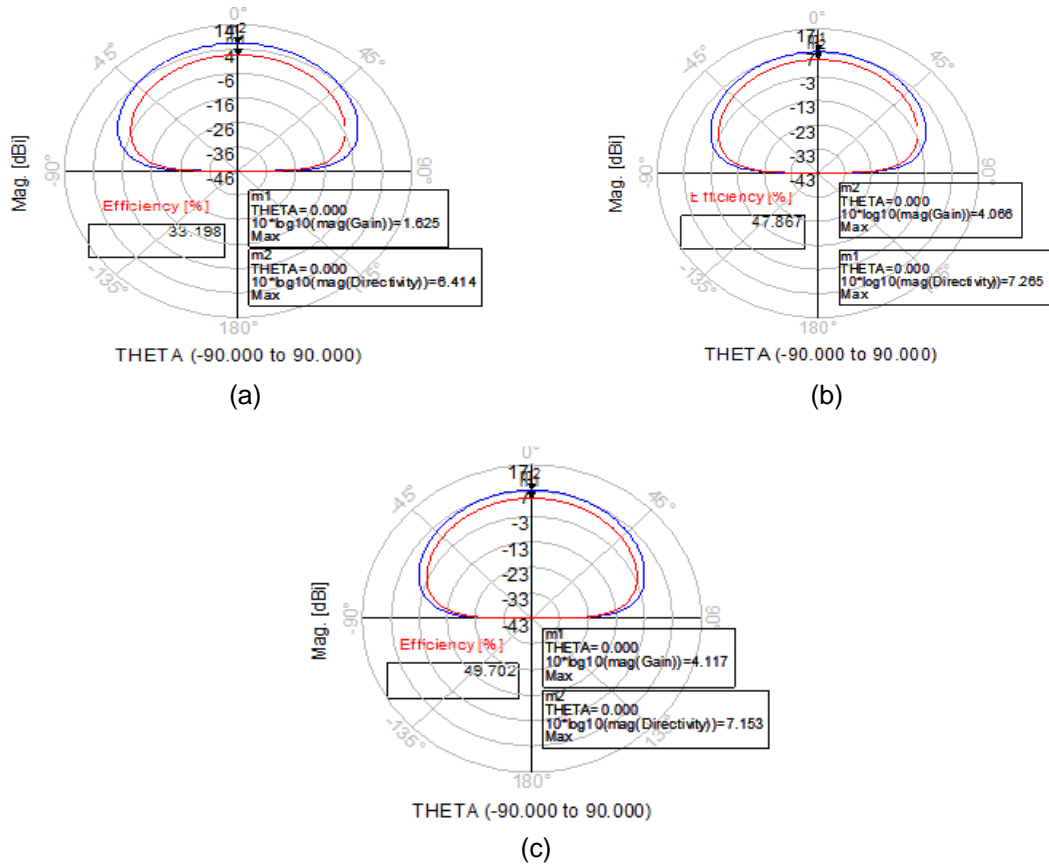


Figure 9. (a) Radiation pattern of conventional MIMO antenna (C-MA) [Model 1], (b) Photograph of MIMO antenna with ring parasitic substrate (RP-MA) [Model 2], (c) Radiation Radiation pattern pattern of MIMO antenna with circular parasitic substrate (CP-MA) [Model 3]

Table 1 summarizes the comparison of conventional MIMO antenna (C-MA) [Model 1], MIMO antenna with ring parasitic substrate (RP-MA) [Model 2], and MIMO antenna with circular parasitic substrate (CP-MA) [Model 3].

Table 1. Comparison of C-MA Antenna, RP-MA Antenna and CP-MA performances

Variables	C-MA	RP-MA		CP-MA	
	[Model 1]	[Model 2]	[Model 2]	[Model 3]	[Model 3]
	Simulated	Simulated	Measured	Simulated	Measured
Center Frequency (GHz)	2.36	2.38	2.36	2.38	2.36
Bandwidth (MHZ)	70	100	100	120	110
Gain (dBi)	1.625	4.066	NA	4.117	NA
Directivity (dBi)	6.414	7.265	NA	7.153	NA
Efficiency (%)	33.9	47.8	NA	49.70	NA
Reflection coefficient (dB)	-12.35	-22.21	-15.93	-23.66	-24.89
Mutual coupling (dB)	-30.924	-28.46	-28.83	-27.59	-31.67
Size	W (mm)	50	50	50	50
	L (mm)	130	130	130	130
	H (mm)	1.6	23.2	23.2	23.2

4. Conclusion

A novel configuration of circular patch MIMO antenna using a ring and circular parasitic radiator structure have been simulated, fabricated, and measured. The C-MA antenna [Model-1] achieves center frequency = 2.36 GHz, bandwidth = 70 MHz, reflection coefficient = -12.35 dB, mutual coupling = -30.92 dB. The RP-MA antenna [Model-2] achieves simulated/measured of center frequency = 2.38 GHz/2.36 GHz, bandwidth = 100 MHz/100 MHz, reflection coefficient =

-22.21 dB/ -15.93 dB, mutual coupling = -28.46 dB/-28.83 dB. The CP-MA antenna [Model-3] achieves simulated/measured of center frequency = 2.38 GHz/2.36 GHz, bandwidth = 120 MHz/110 MHz, reflection coefficient = -23.66 dB/ -24.89 dB, mutual coupling = -27.59 dB/-31.67 dB. A good agreement can be observed between the simulated and measured results, which demonstrates the validity of the design. This result also validates that the addition circular patch MIMO antenna with a ring and circular parasitic radiator structure MIMO could increase bandwidth and gain of MIMO antenna simultaneously. Thus, the proposed MIMO antenna is suitable for LTE application in Indonesia.

Acknowledgments

The work for this grant was supported by the Ministry of Research, Technology and Higher Education, Indonesian Government in Penelitian Kerjasama Perguruan Tinggi (Grand No. 267/UN43.9/PL/K/2016).

References

- [1] Abdulrahman S, Mohd J, Ping S, Guy A, Vandenbosch E. Assessment of PDMS Technology in a MIMO Antenna Array. *IEEE Antennas and Wireless Propagation Letters*. 2016; 15 (1): 1939-1942.
- [2] Ping-Heng K. A glance at FD-MIMO technologies for LTE. *IEEE Wireless Communications*. 2016; 23(1): 2-5.
- [3] Thomas L, Peter T, Frank M. *Evaluation and optimization of LTE MIMO antenna configurations in automotive environment*. The 8th European Conference on Antennas and Propagation (EuCAP). 2014: 1100-1104.
- [4] B Mun, C Jung, MJ Park, B Lee. A Compact Frequency-Reconfigurable Multiband LTE MIMO Antenna for Laptop Applications. *IEEE Antennas and Wireless Propagation Letters*. 2014; 13: 1389-1392.
- [5] Byeongwi M, Changwon J, Myun-Joo P, Byungje L. A Compact Frequency-Reconfigurable Multiband LTE MIMO Antenna for Laptop Applications. *IEEE Antennas and Wireless Propagation Letters*. 2014; 13: 1389-1392.
- [6] Subuh P, Tommi H, Budi S. Performance of Groundplane Shaping in Four-Element Dualband MIMO Antenna. *TELKOMNIKA Telecommunication Computing Electronics and Control*. 2017; 15(1): 220-226.
- [7] Yuli Kurnia N, Rastanto H. Low Mutual Coupling Dualband MIMO Microstrip Antenna Parasitic with Air Gap. *International Journal of Electronics & Communication Technology*. 2014; 12(2): 405-410.
- [8] Leeladhar M, Rajib K, Machavaram V, Kartikeyan. A 2×2 Dual-Band MIMO Antenna with Polarization Diversity for Wireless Applications. *Progress In Electromagnetics Research C*. 2016; 61: 91-103.
- [9] Masoumeh D, Hamid H. *Multiband Uniplanar Monopole Antenna for MIMO Applications*. 20th Iranian Conference on Electrical Engineering (ICEE). Tehran. 2012: 15-17.
- [10] Patil VP. Enhancement of Bandwidth of Rectangular Patch Antenna Using Two Square Slots Techniques. *International Journal of Engineering Sciences & Emerging Technologies*. 2012; 3(2): 1-12.
- [11] R Halappa R, CN Anoop. The Study on Bandwidth Enhancement of Rectangular Microstrip Patch Antenna (RMPA) for Wireless Application. *International Journal of Electronics & Communication Technology*. 2011; 2(4): 171-174.
- [12] S Arun K, K Sunil, DK Srivastava. Design and Bandwidth Enhancement of Rectangular Microstrip Patch Antenna using Double H-Slot Technique for Broadband Applications. *International Journal of Advanced Research in Computer and Communication Engineering*. 2013; 2(12): 4570-4574.
- [13] T Abdurrahim. G-shaped band-notched ultra-wideband MIMO antenna system for mobile terminals. *IET Microwaves, Antennas & Propagation*. 2017; 11(5): 718-725.
- [14] A Raja Abdullah. D Yoharaaj. I Alyani. Bandwidth Enhancement Technique in Microstrip Antenna for Wireless Applications. *PIERS ONLINE*. 2006; 2(6): 633-639.
- [15] T Yingying. Y Liping. Z Xiang. L Changjun. H. Kama. Bandwidth Enhancement of a Printed Slot Antenna with a Diamond-Shaped Tuning Stub. *Progress In Electromagnetics Research C*. 2014; 50: 87-93.
- [16] B Alexander, S Daniel. Gridded Parasitic Patch Stacked Microstrip Antenna with Beam Shift Capability for 60GHz Band. *Progress In Electromagnetics Research B*. 2015; 62: 319-331.
- [17] P Seungbae, K Cheolbok Kim, J Youngho, L Hosang, C Dongki, L Munsoo. Gain enhancement of a microstrip patch antenna using a circularly periodic EBG structure and air layer. *AEU - International Journal of Electronics and Communications*. 2010; 64(7): 607-613.
- [18] T Balakumaran, D Sasidharan. *Design of Microstrip Patch Antenna Array using Parasitic Coupling*. National Conference on Information and Communication Technologies (NCICT). 2015: 30-35.

- [19] P Paritaba, M Balvant, J Me hul. *Bandwidth Enhancement of Microstrip Patch Antenna Using Parasitic Patch Configuration*. International Conference on Communication Systems and Network Technologies. 2012: 53-57.
- [20] A Ramachandran, Puthiyapurayil V Vinesh. Collocated MIMO Antenna with Reduced Mutual Coupling Using Square Ring DGS. *Progress In Electromagnetics Research C*. 2014; 53: 119-125.
- [21] M Mohammad Naser, et.al. Compact EBG Structures for Reduction of Mutual Coupling in Patch Antenna MIMO Arrays. *Progress In Electromagnetics Research C*. 2014; 53: 145-154.
- [22] T Pramendra, P Sharma, T Bandopadhyay. Gain Enhancement of Circular Microstrip Antenna for Personal Communication Systems. *International Journal of Engineering and Technology*. 2011; 3(2): 175-178.
- [23] W Gunawan, et al. Design of triple-band bandpass filter using cascade tri-section stepped impedance resonators. *Journal of ICT Research and Applications*. 2016; 10: 43-56.
- [24] W Gunawan, et al. Multiband bandpass filter (BPF) based on folded dual crossed open stubs. *International Journal of Technology*. 2014; 5: 32-39.
- [25] F Teguh, et al. Multiband RF low noise amplifier (LNA) base on multi section impedance transformer for multi frequency application. *International Journal of Applied Engineering Research*. 2016; 11: 3478-3483.
- [26] K Saidulu, et al. Performance Analysis of Circular Microstrip Patch Antenna With Dielectric Superstrates. *IOSR Journal of Engineering*. 2013; 3(9): 39-51.
- [27] G Wibisono, T Firmansyah. *Design of dielectric resonators oscillator for mobile WiMAX at 2,3 GHz with additional coupling $\lambda/4$* . IEEE Region 10 Conference TENCON. 2011: 489-493.